Vacancy migration at the {410}/[001] symmetric tilt grain boundary of MgO: An atomistic simulation study

D. J. Harris,* G. W. Watson, and S. C. Parker†
Computational Solid State Chemistry Group, School of Chemistry, University of Bath, Claverton Down, Bath BA2 7AY, United Kingdom
(Received 5 May 1997)

We present the results of atomistic simulations to evaluate diffusion pathways and hence activation energies for cation and anion vacancy migration in the MgO {410}/[001] symmetric tilt grain boundary, which can be considered as a series of dislocation pipes. The approach employed in this study is based on molecular dynamics and we found that the diffusion routes were anisotropic with diffusion down the dislocation pipes favored over diffusion between the pipes. The lowest calculated activation energies for isolated vacancies were 1.05 eV for magnesium and 1.01 eV for oxygen at 0 GPa (cf. bulk activation energies of 1.94 eV for magnesium and 2.12 eV for oxygen). The lower activation energies coupled with the enhanced defect concentrations at the interface shows that boundaries are regions of high diffusivity. However, the concentration of vacancy pairs at the interface and the high binding energy of a magnesium-oxygen pair leads to the prediction that a large component of the defects is bound, which in turn causes the activation energy for vacancy migration to approach that of the bulk. In this case the higher boundary diffusivities are the result of high defect concentrations at the boundary. [S0163-1829(97)04442-1]

I. INTRODUCTION

In this paper we describe atomistic simulations used to investigate self-diffusion pathways in MgO at tilt grain boundaries. The diffusion pathways and rates of diffusion along grain boundaries are important for understanding the rheology of polycrystalline phases and as such are vital in understanding processes such as creep.[1]

Atomistic simulations of bulk mineral properties are well established for the prediction of crystal structures,[2,3] and more recently the introduction of free-energy minimization techniques[4] has allowed the inclusion of temperature to study equations of state.[5] Atomistic minimization techniques have also been used to study MgO; Mackrodt and Stewart[6] studied defect formation and migration energies in MgO using static lattice calculations. We have also performed a previous study of defect formation in bulk MgO (Ref. 7), which indicated that the defect formation volume is important and highly dependent on pressure. More recently, Vocadlo *et al.*[8] calculated the activation energies for self-diffusion in MgO as a function of temperature indicating that the energies decreased with increasing temperature while the migration volume increased. These studies have all considered bulk MgO and yet the polycrystalline nature of many materials means that grain boundaries should be considered. These grain boundaries are important for many properties including toughness, fracture strength, and plastic deformation.[9] There is also considerable evidence to suggest that grain boundaries are regions of high diffusivity in ionic crystals. Atkinson and Taylor[10] measured the grain boundary diffusion coefficient in polycrystalline NiO, a compound isostructural with MgO, and found the activation energy to be significantly lower than for bulk diffusion in single-crystal NiO.[11] Duffy and Tasker[12] used computer simulation to calculate the activation energy for single cation vacancy hopping in the {310}/[001] symmetric tilt grain boundary of NiO and also found that the activation energy was lower than that for bulk.

Previous simulations of ionic diffusion along grain boundaries have used static lattice techniques in which the moving ion is systematically fixed at a series of positions while the rest of the cell is allowed to relax around it.[12] However, the difficulty in locating the saddle points and the number of possible pathways that must be considered proved to be time consuming. In this work we use molecular dynamics (MD) to evaluate the formation energies that enables us to estimate the defect concentration and when modified we can use this approach to locate diffusion pathways and activation energies for ion migration. The Schottky defect is the most stable intrinsic defect in MgO because of its dense close packed structure. We therefore considered cation and anion vacancy formation and migration in the {410}/[001] symmetric tilt grain boundary of MgO at 0 GPa. The structure of this grain boundary has not yet been verified experimentally. The nearest system that has been studied is the {310}/[001] tilt boundary of NiO by Merkle and Smith,[13] using high-resolution electron microscopy. They found no evidence for the most stable, low-density boundary which is structurally not unlike our boundary. Later simulation studies[14] suggested that the observed structure was the asymmetric tilt grain boundary, which is less stable than the symmetric tilt. However, we must be cautious of a too detailed comparison because NiO, unlike MgO is easily oxidized and hence the boundary of NiO is likely to contain nickel vacancies and holes as suggested for the free surfaces.[15] The {410} grain boundary of MgO was chosen for several reasons. First, MgO is an important ceramic and mineral (believed to be a significant component of the lower mantle). Second, it is a simple face-centered-cubic crystal, which makes it ideal as a model system. Third, previous calculations have been carried out for bulk MgO, which can be utilized for determining the validity of our approach. Finally, we have previously modeled the {410} grain boundary as a function of pressure[16]

using lattice dynamics which has identified reasonable starting configurations for the MD simulations.

II. METHODS

The initial calculations of the pure {410} grain boundary were carried out using the MD code QCTPMD (Refs. 17, 18, 19) within the isobaric, isothermal ensemble (NPT). This technique allows us to directly solve Newton's laws of motion for a periodically repeating box of ions over a finite time span. The Nosé-Hoover constant-temperature method[20,21,22] places the cell in contact with a heat bath allowing energy to transfer into or out of the cell ensuring that a constant-temperature ensemble is obtained. The constant pressure method of Parrinello and Rahman[23] allows a dynamical change in both the lattice vectors and angles with time. Initially the ions are assigned random velocities such that the system starts out with the desired simulation temperature but such that the cell has no translational momentum.

The molecular dynamics proceeds by using the forces calculated from a potential model to update the velocity and position of the ions by solving Newton's laws of motion numerically, in our case using a fifth-order predictor corrector method due to Gear.[24] A time-step of 10^{-15} s was used that allowed simulations of the order of 10^{-11} s (10 ps) for each possible defect configuration. The velocities of the ions were scaled to the simulation temperature before the data collecting run was performed to ensure that the cell had reached equilibrium. In addition, we included corrections to the Ewald method,[25] as described by Leslie and Gillan,[26] which allows calculation of charged simulation cells. This enables us to evaluate the thermally averaged formation energies.

As noted above, one of the aims of this work was to calculate the diffusion pathways and activation energies for vacancy migration. The difficulty in using traditional molecular dynamics is that the activation energies for ion migration in solids are often much greater than the thermal energy available and hence the pathway and activation energy cannot be identified except at very high temperatures and by using extremely long runs, as has been elegantly exemplified by Meyer and co-workers.[27] We chose a different route not least because we also wanted an approach that could calculate the activation energies and migration properties both for the slowest moving species, which is required for modeling creep, and at low temperatures where thermal energies will not be sufficient to obtain significant atomic transport. Thus we have modified the MD code to directly calculate diffusion pathways and activation energies. This was achieved by setting up the simulation cell such that there was one vacancy per cell and applying a small force to an adjacent ion in the direction of the vacancy. A force was only added to ensure that the net force on the moving ion always contained a small component in the direction of the vacancy, thus moving it toward the vacancy but also allowing any perpendicular movement. A counterforce equal but in the opposite direction was added to the remaining ions to ensure no translational momentum was added to the cell. In addition, the volume was kept constant at the volume obtained from the MD simulation described above under NPT conditions and the velocities of the ions were scaled each step to ensure that no net energy was added to the system from the applied forces. When comparing with the static calculations the chosen temperature of the MD cell was 10 K. Furthermore, the force was sufficiently small so that the simulation time to complete the jump was in excess of 10^{-12} s to allow sufficient vibrations for the rest of the crystal to relax back around the ion. Thus we are simply allowing the crystal to relax as the ion moves from one site to another such that the pathway perpendicular to a line joining the starting and finishing positions is not constrained.

The forces between the ions are evaluated at each time step using interatomic potentials which comprise of terms describing Coulombic and short-range interactions. Two potential models, those of Sangster and Stoneham (SS) (Ref. 28) and Lewis and Catlow (LC) (Ref. 29), were chosen to provide a check on the sensitivity of the results to the details of the potential parameters and give an estimate of the confidence we can have in the final energies. These potentials differ in the values of the parameters in the analytical expressions used to describe the short-range interactions of the form

$$V(r_{ij}) = A_{ij}\exp\left(\frac{-r_{ij}}{\rho_{ij}}\right) - \frac{C_{ij}}{r_{ij}^6}, \tag{1}$$

where A, ρ, and C are the adjustable parameters and r_{ij} is the interionic separation. In addition these potentials normally incorporate a shell model[30] to simulate the electronic polarizability of the ions. However, the large size of the grain-boundary simulation cell and number of pathways meant that the rigid-ion model was used.

Before modeling the diffusion pathway we evaluated the grain-boundary structure using both potential models.

III. RESULTS AND DISCUSSION

A. Vacancy formation at the interface

The simulations reported here required cells of 960 atoms to minimize defect-defect interactions. Table I shows the partial Schottky energies calculated using the rigid-ion and shell models for the SS and LC potentials for the sites indicated in Fig. 1. The Schottky energy is defined as the energy required to create (in the case of MgO) a pair of vacancies and place the ions at the bulk edge, forming new crystal. To simplify the presentation of the results we have defined partial Schottky energies as the energy to remove a single ion and add it to the bulk. The bulk energy of a single ion is its total interaction energy in a perfect crystal. Thus the bulk Schottky energy is simply the sum of the Mg and O bulk partial Schottky energies. The results in Table I show that the two different models (LC and SS) gave the same trends and similar results with the LC model giving consistently higher energies than the SS model by about 0.3 eV. In each case the rigid-ion potentials gave slightly higher energies than the corresponding shell potentials for each vacancy position again by about 0.3 eV. Finally, the MD and static lattice calculations again show the same trends but differ slightly because the MD cell volume was fixed at the calculated 300 K cell dimensions. The good level of agreement between the

TABLE I. Cation and anion partial Schottky energies for the {410} tilt grain boundary of MgO calculated using static lattice energy minimization with the rigid-ion and shell-model versions of the Lewis-Catlow (LC) and Sangster-Stoneham (SS) potentials and using molecular dynamics (MD) with the rigid ion Lewis-Catlow potential.

	Partial Schottky energies (eV)				
Vacancy position (Type)	MD (300 K) LC (ri)	Static energy minimization (without temperature) LC (ri)	LC (sh)	SS (ri)	SS (sh)
A (Mg)	3.32	3.53	3.26	3.30	3.09
B (Mg)	3.81	4.11	3.73	3.90	3.60
C (Mg)	3.92	4.21	3.84	3.97	3.68
D (Mg)	3.31	3.69	3.24	3.41	3.07
E (Mg)	4.61	4.99	4.40	4.84	4.40
Bulk (Mg)	3.63	4.16	3.55	3.92	3.47
A (O)	3.77	3.97	3.75	3.63	3.44
B (O)	4.21	4.44	4.35	4.15	4.02
C (O)	4.35	4.59	4.37	4.27	4.07
D (O)	3.71	4.05	3.96	3.68	3.59
F (O)	4.99	5.34	5.10	5.11	4.92
Bulk (O)	4.08	4.62	4.27	4.24	3.99

models for the relative stabilities of the sites suggests it is reasonable to use the rigid-ion model for evaluating an activation energy, which is again a relative stability. Additionally, we have continued with the LC potential because it is the most compatible with silicate potentials such as THB1 (Ref. 4), and will therefore allow direct comparison when we begin to study heteroepitaxial interfaces, i.e., for diffusion between grains of different composition.

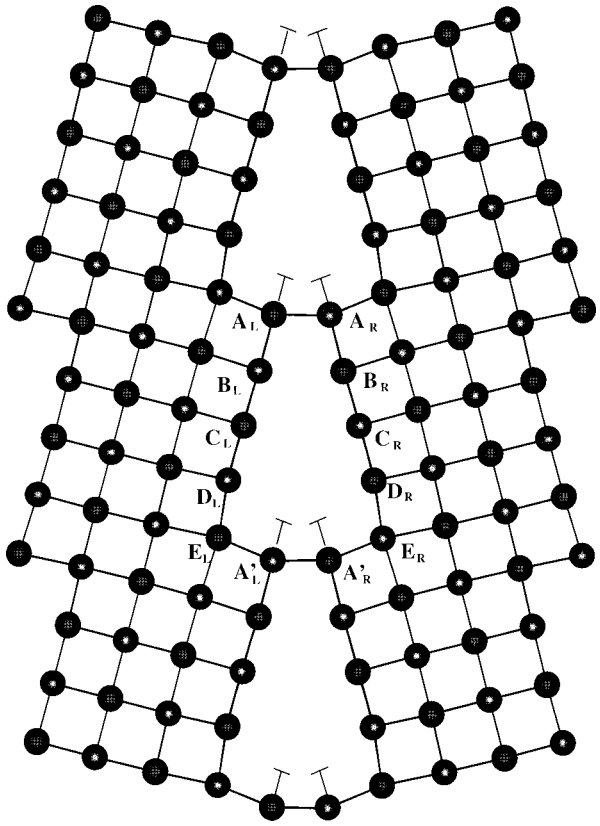

FIG. 1. The minimized structure of the {410} tilt grain boundary of MgO showing the dislocation pipes and labeling the positions of the vacancy sites along the boundary.

The positions marked *A* and *D* in Fig. 1 have the lowest partial Schottky energies for both cation and anion vacancies with approximately equal energies. In addition, these energies are lower than those for the bulk. For example, the partial Schottky energy for magnesium vacancies is 3.53 eV at site *A* and 3.69 eV at site *D* compared to a bulk value of 4.16 eV using the LC rigid-ion potential.

The low Schottky energies found at the boundary compared to the bulk suggests that vacancy concentrations will be greater at the boundary than in bulk MgO. As the relative diffusivity in the bulk and at the boundary depend on the relative concentration of mobile species, we need a quantitative estimate of the relative defect concentrations. In addition, as we are considering charged species, the calculation of the relative defect concentrations should also include a treatment of the space charge because these are charged defects and hence we follow the work given by Duffy and Tasker[31] for the determination of space-charge effects. These relationships are briefly summarized below. For a bulk crystal with N sites available for vacancy formation, the fraction of bulk sites occupied (n_0) by vacancies to sites available is given by

$$\frac{n_0}{N} = \exp\left[-\left(\frac{F^{\mathrm{Mg}} + F^{\mathrm{O}}}{2kT}\right)\right], \tag{2}$$

where F^{Mg} and F^{O} are the bulk partial Schottky energies. The fraction of sites (n_b) occupied at a grain boundary with N_b available low-energy sites in the boundary plane is given by

$$\frac{n_b}{N_b} = \left(\frac{n_0}{N}\right)\exp\left(-\left[\frac{F_{\mathrm{I}}^{\mathrm{Mg}} + F_{\mathrm{I}}^{\mathrm{O}}}{2kT}\right]\right)(1+\delta), \tag{3}$$

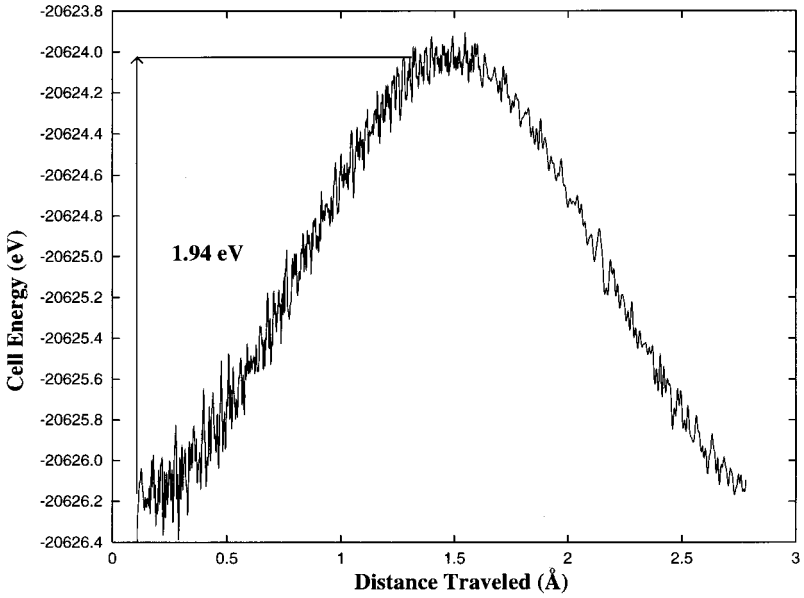

FIG. 2. Energy profile for diffusion of a magnesium vacancy in bulk MgO as a function of distance traveled.

where $F_I^{Mg}=F_B^{Mg}-F^{Mg}$ and $F_I^{O}=F_B^{O}-F^{O}$ (F_B^{Mg} and F_B^{O} are the boundary partial Schottky energies), and δ is given by

$$\delta=\frac{\left\{2\kappa^{-1}\left(\frac{N}{N_b}\right)\exp\left[\frac{F_I^{Mg}}{2kT}\right]\sinh\left[\frac{F_I^{Mg}-F_I^{O}}{4kT}\right]\right\}}{\left\{1+\kappa^{-1}\left(\frac{N}{N_b}\right)\exp\left[\frac{F_I^{Mg}+F_I^{O}}{2kT}\right]\cosh\left[\frac{F_I^{Mg}-F_I^{O}}{4kT}\right]\right\}}, \tag{4}$$

where κ^{-1} is the screening length given by

$$\kappa^{-1}=\left(\frac{\varepsilon_0\varepsilon kT}{2e^2n_0}\right)^{1/2}. \tag{5}$$

For the purposes of this treatment only the A site in the {410} boundary is considered here. For our simulation cell N is 5.4×10^{28} m^{-3} and N_b is 2.7×10^{18} m^{-2}, thus at 1500 K 11.4 times as many boundary sites were occupied than bulk sites which will cause a similar enhancement in diffusivity. This may be further modified by the difference in the relative activation energies for migration that is discussed in the following sections.

Furthermore, the results suggest that there will be equal concentrations of cation and anion vacancies. Therefore we considered bound magnesium-oxygen vacancy pairs at the grain boundary which may affect the migration properties of the vacancies. We found a large binding energy, 2.83 eV, which resulted in a boundary to bulk defect concentration ratio of 6.30×10^5, much higher than that calculated for isolated vacancies at the boundary.

In summary, there will be an enhancement of vacancies at the boundary but the large binding energies suggest they will be largely bound.

B. Diffusion path for isolated vacancies in the bulk

Previous calculations on diffusion properties have used static lattice calculations in which the moving ion is held fixed at the point estimated to be the saddle point of the migration while the rest of the cell is allowed to relax around it. Using this method, Mackrodt and Stewart[6] calculated activation energies for vacancy migration of 2.16 eV for magnesium and 2.38 eV for oxygen in bulk MgO. More recent calculations using the SS potential[28] by Vocadlo *et al.*[8] predicted activation energies of 1.99 eV for magnesium and 2.00 eV for oxygen. Experimental activation energies for magnesium vacancy migration are available, which include values of 2.28 eV (Ref. 32) and 1.57–3.46 eV.[33] In addition, NMR relaxation times have been used to estimate activation energies at 800 °C. This gives rise to 2.00 eV and 1.56 eV for oxygen and magnesium, respectively.[34] However, comparison of data from NMR relaxation with activation energies is difficult.[34]

In order to test the viability of our approach we initially calculated diffusion pathways and activation energies for cation and anion vacancy migration in bulk MgO. The rest of the crystal was kept at 10 K, using velocity scaling allowing the ions to relax around the moving ion. A plot of the lattice energy of the cell with respect to the distance travelled by the moving magnesium vacancy is shown in Fig. 2. This gave an activation energy of $1.94+/-0.1$ eV for magnesium diffusion while the oxygen activation energy was calculated to be $2.12+/-0.1$ eV. These energies are approximate since the saddle-point energy was estimated from the thermal average of the MD energies such as those shown in Fig. 2. Within the accuracy of these estimates the bulk activation energies can therefore be considered identical. These energies compare favorably with the experimental and calculated data. Examination of the pathway taken by the migrating vacancy showed that it followed a linear route between the two sites diagonally across the face of an MgO cube, which agreed with the approximately room-temperature data calculated by Vocadlo *et al.*[8] We now apply this approach to modeling diffusion at the grain boundary.

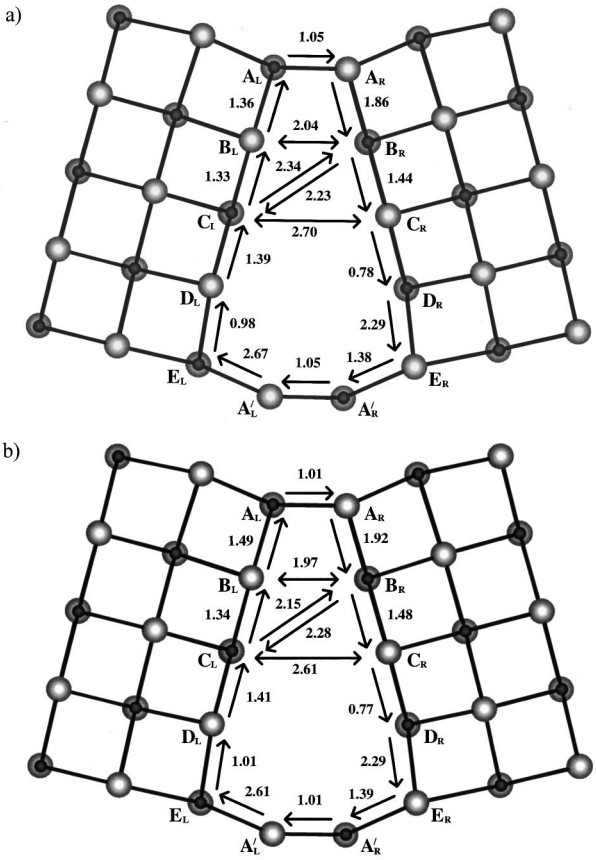

FIG. 3. The activation energies for (a) magnesium and (b) oxygen vacancy migration at the grain boundary.

C. Diffusion path for isolated vacancies at a grain boundary

Diffusion at the boundary was modeled first by introducing isolated vacancies along the boundary. An ion of the same type as the vacancy from a neighboring site was then pushed towards this vacancy. A grain boundary can be described as a series of dislocation pipes, as illustrated in Fig. 1, and it is clear that even for a simple boundary like the {410}/[001] there are a number of diffusion pathways for vacancy migration. We report the two lowest-energy mechanisms for diffusion along the boundary. These are for diffusion (1) between the dislocation pipes, defined as diffusion along the same side of the boundary without travelling to the opposite surface, for example between sites B_R and C_R (Fig. 1), and (2) down the dislocation pipes as a result of diffusion from one side of the grain boundary to the opposite surface, for example between sites A_R and A_L (Fig. 1), which occurs perpendicular to the plane of the figure. Note that positions A and A' on the figure legend are equivalent sites.

Figure 3(a) shows the direction of travel and associated activation energies for magnesium vacancy hopping in the {410} boundary while Fig. 3(b) shows the energies for oxygen vacancies. The energies are very similar in both cases with less than a 0.1 eV variation between corresponding activation energies. Thus for brevity, unless otherwise stated, only the energies and trends for magnesium vacancies are described in the following sections.

1. Diffusion between the dislocation pipes

Diffusion between the pipes resulted in activation energies which in most cases were lower than those calculated for bulk. The exception was for vacancy migration to the least stable vacancy site E from sites D and A'. Generally, it was found that the activation energy for migration was lower when moving to a more stable site than to a less stable site. The activation energies for magnesium to the D site from C and E were $0.78+/-0.1$ eV and $0.98+/-0.1$ eV, respectively. Migration away from the D site required energies of $1.39+/-0.1$ eV and $2.29+/-0.1$ eV to the C and E sites, respectively, indicating that a vacancy would not only be attracted but also bound to this site. Thus the overall activation energy for migration between pipes is 2.29 eV, which is slightly greater than the bulk value of 1.94 eV.

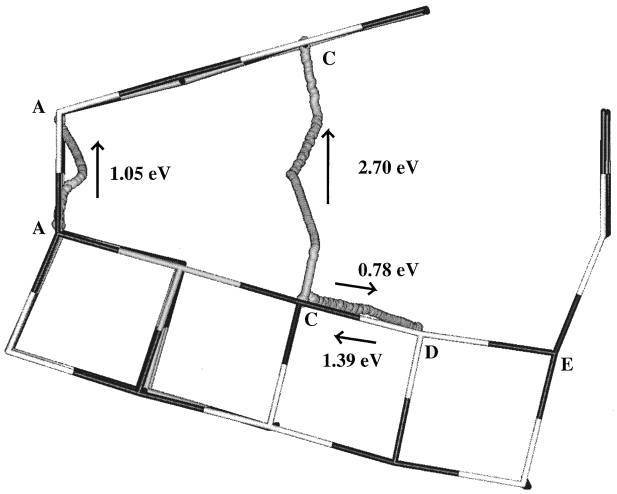

FIG. 4. Diffusion pathway for magnesium diffusion between various sites in the {410} tilt grain boundary of MgO.

Animation of the ions in the simulation allowed us to investigate the diffusion pathway along the grain boundary (Fig. 4). We found that the moving ion did not take the direct route between two sites but rather a curved trajectory. The point which deviated to the greatest extent from the direct path corresponded to the saddle point and was closest to the center of the grain boundary, for example during diffusion from the C to the D site the moving ion moved approximately 0.1 Å into the grain boundary. The nonlinear trajectory occurred for all of the diffusion routes modeled, a result similar to that found by Duffy and Tasker[12] for cation vacancy migration in the {310} tilt grain boundary of NiO and illustrates the difficulty static simulations had in locating saddle points. A plot of the lattice energy of the cell with respect to the distance travelled by the moving magnesium vacancy for diffusion between sites C and D at 0 GPa is shown in Fig. 5, illustrating the smooth progression of the ion and the calculation of the activation energies for the forward and reverse processes.

2. Diffusion down the dislocation pipes

The most favorable pathway for diffusion down the dislocation pipes involved vacancy hopping between A_L and A_R, which required an activation energy of $1.05+/-0.1$ eV. The diffusion pathway showed that a curved route was followed for migration from A_L to A_R, which is shown in Fig. 4. Vacancy migration became more unfavorable where the distance to be crossed was larger and resulted in

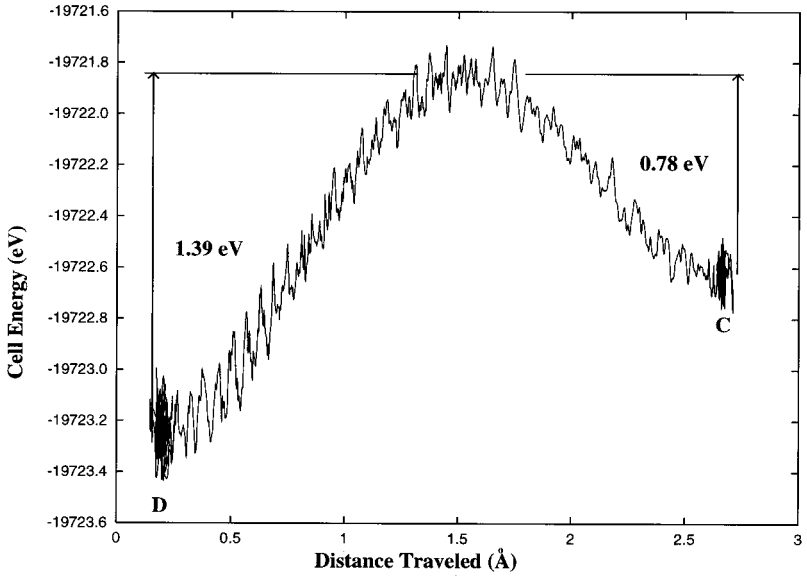

FIG. 5. Energy profile for diffusion of a magnesium vacancy between positions C and D in the {410} tilt grain boundary of MgO as a function of distance traveled.

larger activation energies of $2.00+/-0.1$ eV and $2.70+/-0.1$ eV. Diffusion from sites C_L to C_R also followed a slightly curved route as the moving ion was influenced by neighboring ions (Fig. 4).

In summary, the diffusion process is anisotropic with diffusion down the dislocation pipes in the [001] direction, with an activation energy of $1.05+/-0.1$ eV, preferred to diffusion between the pipes, with an activation energy of $2.29+/-0.1$ eV. This agrees with the experimental work of Stubican and Osenbach,[35] who studied chromium diffusion in oxide boundaries including MgO, and of Turnbull and Hoffman[36] who looked at silver bicrystals. In addition, the activation energies were much lower than in the bulk, which agrees with the relationship found in experimental studies of diffusion in polycrystalline NiO by Atkinson and Taylor[10] who measured an activation energy of 1.78 eV compared to the value of 2.5 eV measured for bulk diffusion in single-crystal NiO.[11]

D. The mobility of bound defects

The calculations presented suggest enhanced diffusion rates are obtained at the grain boundary as a result of the lower activation energies and increased free vacancy concen-

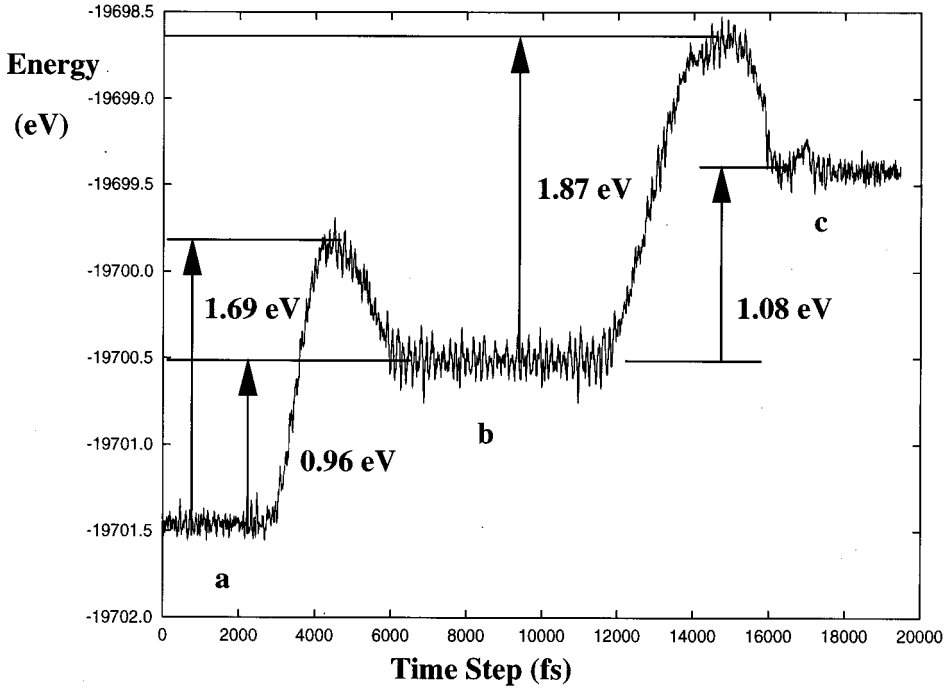

FIG. 6. Energy profile for diffusion of a bound magnesium vacancy between positions A_R and A_L in the {410} tilt grain boundary of MgO as a function of time step demonstrating the change in binding energy between (a) nearest-neighbor, (b) second-nearest-neighbor, and (c) third-nearest-neighbor positions.

trations which agrees with the MD study in the {310}/[001] NiO tilt grain boundary.[27] However, the binding energies of the vacancy pairs are high and depending on the preparation conditions the boundary might be dominated by bound defects. On evaluating the activation energy for vacancy migration from A_L to A_R for a magnesium vacancy, which is initially bound as a function of separation of the pair to the second and third nearest neighbor positions, e.g., Fig. 6, the highest activation energy of $1.87+/-0.1$ eV was obtained for separation to the third-nearest-neighbor position. This is higher than the single vacancy activation energy of $1.05+/-0.1$ eV and closer to the bulk value of $1.94+/-0.1$ eV. As the diffusivity is related to the product of defect concentration and $\exp(-E_{\rm act}/RT)$ the calculations imply that when the boundary contains a large number of defects they will be bound and the high diffusivity will be controlled by the enhanced number of diffusing species rather than any lowering of the activation energy.

IV. CONCLUSIONS

We have demonstrated that the ability of relaxation via modified molecular dynamics is a useful tool for predicting the pathways when the activation energies are too high to be accessed using MD within an ensemble. The diffusion was found to be anisotropic with diffusion down the dislocation pipes more favorable than diffusion between the pipes. Activation energies for hopping of isolated magnesium and oxygen vacancies down the dislocation pipes forming the grain boundary was found to have a lower activation energy than that for bulk diffusion, which agreed with experimental observations of NiO.[10,11] The lower density of the grain boundary compared to the bulk allows the diffusing ion to follow a curved trajectory into the boundary.

Defect calculations have shown two low-energy vacancy sites were found in the grain boundary at positions *A* and *D*. Site *D* has a similar geometry to the lowest-energy site found by Duffy and Tasker[12] in the {310} tilt grain boundary of NiO. The low boundary vacancy energies suggest there will be high vacancy concentrations at the boundary and that they will be bound. Moreover, the activation energy of bound defects is close to the bulk value and hence the enhanced defect concentration due to the low vacancy formation energies gives rise to high diffusion coefficients for the boundary migration. This result has already been suggested, albeit in a different material, by Wuensch and Tuller[37] who observed that the activation energy for Ni^{2+} diffusion at grain boundaries of ZnO was similar to that of the bulk and the increased diffusivity was attributed to the enhanced carrier concentration at the boundary. Furthermore, if the orientation of the dislocation pipes was such that the migrating species had to move between them then the observed grain boundary activation energy would appear higher than that of the bulk.

Future work will extend the application of this program to model diffusion at high pressure and in other grain boundaries and boundaries between other mantle forming minerals such as SiO_2 stishovite, $MgSiO_3$ perovskite. In addition, we also intend to consider heterointerfaces, i.e., between different mineral grains and the effect that adding impurities such as calcium and iron has upon the diffusion.

ACKNOWLEDGMENTS

D.J.H. and S.C.P. would like to thank the N.E.R.C. for financial support and we would all like to thank the E.P.S.R.C. for financial support and Biosym/MSI for the use of their Insight II program.

*Electronic address: d.harris@bath.ac.uk

†Electronic address: s.c.parker@bath.ac.uk URL:http://www.bath.ac.uk/~chsscp/group/group.html

[1] J. P. Poirier, *Creep of Crystals* (Cambridge University Press, Cambridge, 1985).

[2] C. R. A. Catlow, J. M. Thomas, S. C. Parker, and D. A. Jefferson, Nature (London) **295**, 658 (1982).

[3] S. C. Parker, Solid State Ion. **8**, 179 (1983).

[4] S. C. Parker and G. D. Price, Adv. Solid State Chem. **1**, 295 (1989).

[5] A. Wall, S. C. Parker, and G. W. Watson, Phys. Chem. Miner. **20**, 69 (1993).

[6] W. C. Mackrodt and R. F. Stewart, J. Phys. C **12**, 431 (1979).

[7] D. R. Mills, S. C. Parker, and A. Wall, Philos. Mag. A **64**, 1133 (1991).

[8] L. Vocadlo, A. Wall, S. C. Parker, and G. D. Price, Phys. Earth Planet. Int. **88**, 193 (1995).

[9] *Grain Boundary Phenomena in Electronic Ceramics*, edited by L. M. Levinson (American Ceramic Society, Columbus, OH, 1981).

[10] A. Atkinson and R. I. Taylor, Philos. Mag. A **43**, 979 (1981).

[11] A. Atkinson and A. E. Hughes, Philos. Mag. A **43**, 1071 (1981).

[12] D. M. Duffy and P. W. Tasker, Philos. Mag. A **54**, 759 (1986).

[13] K. L. Merkle and D. J. Smith, Phys. Rev. Lett. **59**, 2887 (1987).

[14] J. H. Harding, S. C. Parker, and P. W. Tasker, in *Non-Stoichiometric Compounds Surfaces, Grain Boundaries and Structural Defects*, edited by J. Nowotny and W. Weppner (UKAEA, Harwell, 1989).

[15] P. M. Oliver, S. C. Parker, and W. C. Mackrodt, Mod. Simul. Mater. Sci. Eng. **1**, 755 (1993).

[16] D. J. Harris, G. W. Watson, and S. C. Parker, Philos. Mag. A **74**, 407 (1996).

[17] M. Matsui, J. Chem. Phys. **91**, 489 (1989).

[18] G. W. Watson, S. C. Parker, and A. Wall, J. Phys.: Condens. Matter **4**, 2097 (1992).

[19] G. W. Watson, A. Wall, and S. C. Parker, Phys. Earth Planet. Int. **89**, 137 (1995).

[20] W. G. Hoover, Phys. Rev. A **31**, 1695 (1985).

[21] S. Nosé, J. Chem. Phys. **81**, 511 (1984).

[22] S. Nosé, J. Phys.: Condens. Matter **2**, SA115 (1990).

[23] M. Parrinello and A. Rahman, J. Appl. Phys. **52**, 7182 (1981).

[24] C. W. Gear, *Numerical Initial Value Problems in Ordinary Differential Equations* (Prentice-Hall, Englewood Cliffs, NJ, 1971).

[25] P. P. Ewald, Ann. Phys. (Leipzig) **64**, 253 (1921).

[26] M. Leslie and M. J. Gillan, J. Phys. C **18**, 973 (1985).

[27] M. Meyer, T. Karakasidis, and C. Waldburger, Mater. Sci. Forum **207-209**, 525 (1996).

[28] M. J. L. Sangster and A. M. Stoneham, Philos. Mag. B **43**, 597 (1981).

[29] G. V. Lewis and C. R. A. Catlow, J. Phys. C **18**, 1149 (1985).

[30] B. G. Dick and A. W. Overhauser, Phys. Rev. **112**, 90 (1958).
[31] D. M. Duffy and P. W. Tasker, Philos. Mag. A **50**, 143 (1984).
[32] D. R. Sempolinski and W. D. Kingery, J. Am. Ceram. Soc. **63**, 664 (1980).
[33] R. Freer, J. Mater. Sci. **15**, 803 (1980).
[34] P. S. Fiske, J. F. Stebbins, and I. Farnan, Phys. Chem. Miner. **20**, 587 (1994).
[35] V. S. Stubican and J. W. Osenbach, Solid State Ion. **12**, 375 (1984).
[36] D. Turnbull and R. E. Hoffman, Acta Metall. **2**, 419 (1954).
[37] B. J. Wuensch and H. L. Tuller, J. Phys. Chem. Solids **55**, 975 (1994).